CHARACTERIZATION OF INCLINED GAS JETS IN TWO-PHASE CROSSFLOW

A.M.S. Suarez
J.B.R. Loureiro
A.P. Silva Freire

Mechanical Engineering Program (PEM/COPPE/UFRJ), C.P. 68503, Rio de Janeiro, 21941-972,Brazil

Abstract: *The purpose of the present work is to study the behavior of inclined gas jets in vertical upward liquid flows. Three different angles of injection (α = -45°, 0°, 45°) are studied for four different gas flow rates (1, 2, 3 and 4 m^3h^{-1}) and four liquid flow rates (2, 3, 4 and 5 m^3h^{-1}). The experimental apparatus consists of a closed vertical loop with a test section 10 meters in length and 44 mm in internal diameter. Measurements were obtained for pressure drop and flow pattern. A special set of pneumatic fast-closing valves was devised to account for the pressure drop due to gravitational effects. The Shadow Sizing technique was used for flow visualization. The present results clarify the effects of the gas injection configuration on the pressure drop along the pipe and identify the morphological structure of the flow for every experimental condition.*

Keywords: *turbulence, gas injection, two-phase flow, lift technique.*

1. INTRODUCTION

Gas injection into a vertical pipe is a commonly used technique to reduce pressure head on producing wells (Guet (2004), Saepudin et al. (2007)). The principle is very simple: the injected gas decreases the average density of the mixture, resulting in a lower gravitational pressure drop.

The absence of moving parts and the great flexibility of the technique in dealing with multicomponent mixtures offer particular attractiveness in applications. The variety of existing installations include continuous or intermittent gas injection by single or multiple nozzles.

The purpose of the present work is to study the effects of the angle of injection – counter-current, orthogonal, co-current – on the total pressure loss provoked by a single injector. The pressure losses are the result of four combined effects: gravity, acceleration, wall friction and bubble agitation (gas-liquid interaction). Depending on the angle of injection the relative contributions of these four effects change, yielding combinations that contrary to the expected may result in an increase of pressure drop. Unexpected physical behavior has previously been observed in other phenomena. For example, in oil-water flows the phenomenon of phase inversion has been observed to induce high wall friction and thus a high pressure gradient (Brauner (1998), Descamps et al. (2006)).

In the present work, an experiment is specially devised to separately account for the gravity, wall friction and acceleration (with bubble agitation) contributions on pressure drop for a variety of liquid and gas flow rates and angle of injection. Three different angles (α) are tested -45° (counter-current), 0° (orthogonal) and 45° (co-current).

The results show that the benefits of the high decrease in pressure due to the gravity effects are counteracted by the high pressure increase provoked by the acceleration of the gas and the turbulent agitation.

2. EXPERIMENTS

The experiments were carried out in a vertical 2"pipe for four different gas flow rates (1, 2, 3 and 4 m^{3}h^{-1}) and four liquid flow rates (2, 3, 4 and 5 m^{3}h^{-1}). The injection nozzle was 2 mm in diameter and is referred in the following as being located at z = 0. To measure the total pressure drop, pressure taps were set 50 cm upstream and downstream of the injection point.

The liquid and gas flow rates were measured with a Endress+Hauser magnetic flow meter a calibrated rotameter. The pressure difference was measure with a differential transducer.

The general experimental set up is shown in Fig. 1. Four valves were used to measure the gas hold-up. An automatic pneumatic system was used to simultaneously close the gas supply valve (V4) and the two valves in the test section (V1 and V3). A forth valve (V2) was also activated to open the by-pass section and ensure a constant liquid flow rate in the system.

3. GENERAL FLOW CONFIGURATIONS

The flow configurations for the three distinct injection angles (α = -45°, 0°, 45°) were characterized through a Dantec Shadow Sizer System.

Figures 2 through 4 show the flow patterns for one liquid flow rate (Q_l = 2 m^{3}h^{-1}) and four gas flow rates (Q_g = 1, 2, 3 and 4 m^{3}h^{-1}).

For the lowest Q_g (= 1 m^{3}h^{-1}), the buoyance effects soon take over yielding a flow pattern dominated by large bubbles. The inclined injectors tend to induce the formation of large bubbles that quickly migrate to the centre pipe
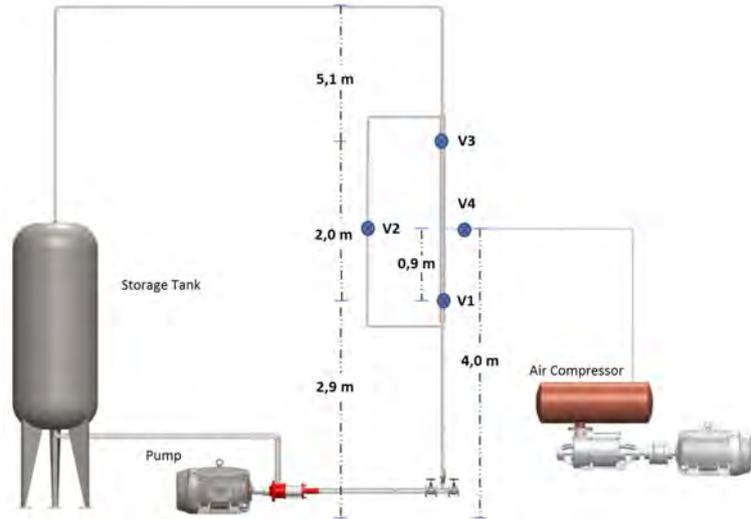
Figura 1: Experimental set up for the gas-lift experiments.

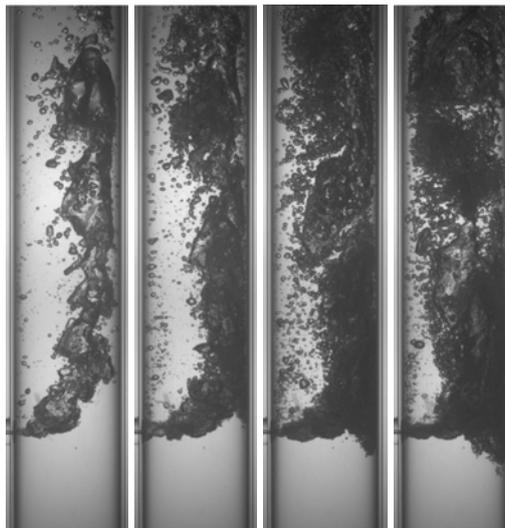Figura 2: General flow configuration for counter-current injection. $Q_l = 2$ m^{3}h^{-1} and $Q_g = 1, 2, 3$ and 4 m^{3}h^{-1}.

Figura 3: General flow configuration for orthogonal injection. $Q_l = 2$ m^{3}h^{-1} and $Q_g = 1, 2, 3$ and 4 m^{3}h^{-1}.

region. The orthogonal gas injection causes the bubbles to hit the upper wall, resulting in a pattern that is skewed to the far (impinging) wall.

For $Q_g = 2$ m^{3}h^{-1}, the flow dynamics is completely different. The momentum of the injected gas is large enough to dominated in a short distance over the buoyance and acceleration effects. Thus, irrespective of the jet angle, the injected bubbles are smashed against the opposite wall resulting in a distribution of bubbles with smaller diameters. For the
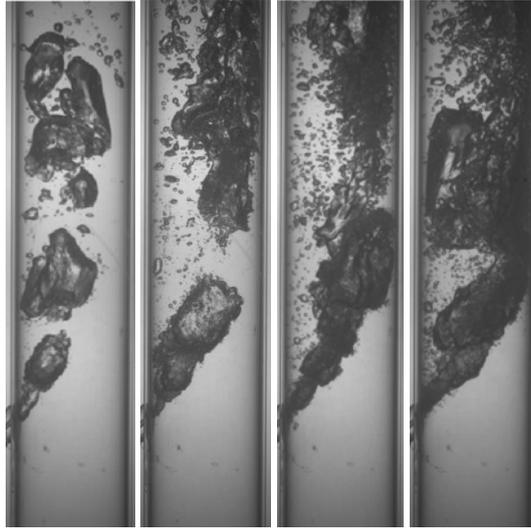
Figura 4: General flow configuration for co-current injection. Q_l = 2 m^{3}h^{-1} and Q_g = 1, 2, 3 and 4 m^{3}h^{-1}.

negative angle, at about one pipe diameter downstream of the injection point (located at $z = 0$) the bubbles almost fill the entire diameter span. For $\alpha = 0^o$ and 45°, the bubbles are dislocated to the impinging wall side.

For the two higher injection rates (Q_g = 3 and 4 m^{3}h^{-1}) and α = -45°, the jet impact on the wall, together with the high shear and turbulence, provoke a strong bubble break up that results in the appearance of a swarm of small bubbles. For Q_g = 4 m^{3}h^{-1} the injected gas penetrates a distance of about two pipe diameters upstream of $z = 0$ before the buoyance and main flow interaction effects win over the injected momentum, causing the gas to change direction and move up. Very close downstream of $z = 0$ the bubbles are observed to occupy most of the pipe cross area.

For the other two injection angles ($\alpha = 0^o$, 45°), at short distances from $z = 0$ the bubbles tend to concentrated on the right-half of the pipe. At about $z = 2$D the bubbles spatial distribution is more even, occupying most of the pipe cross section.

An analysis of the flow configurations for the highest liquid flow rate (Q_l = 5 m^{3}h^{-1}) and four gas flow rates is presented next. Figures 5 through 7 illustrate the experimental results. Compared to the previous discussion, the flow pattern are now completely different.
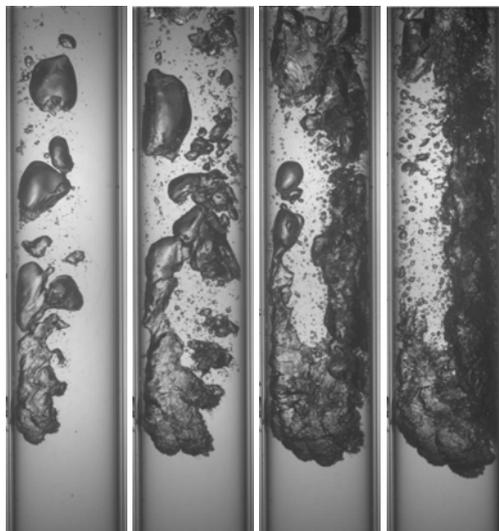

Figura 5: General flow configuration for counter-current injection. Q_l = 5 m^{3}h^{-1} and Q_g = 1, 2, 3 and 4 m^{3}h^{-1}.

For the lowest Q_g the gravity and acceleration effects soon dominate the momentum of the injected gas, pushing the bubbles up to an adjacent region to the near wall; at a distance $z = 3$D the large bubbles are still skewed left for all three injection angles. For Q_g = 2 m^{3}h^{-1}, the flow resulting from the inclined nozzles (α = -45°, 45°) seems to facilitate the formation of large bubbles. The orthogonal injection, on the other hand, seems to expose the bubbles to flow conditions (shear stress and turbulence) that results in a relatively well organized bubble plume. The effects of bubble impingement on the facing wall is apparent for the injection rates Q_g = 3, 4 m^{3}h^{-1}. The impact appears to reduce the size of bubbles yielding a diameter distribution with smaller bubbles. For both the inclined angles, the issuing jet does not impact directly on the opposite wall but rather interacts directly with the oncoming flow. The relative organization of the flow for the inclined injection angles is thus much different from the orthogonal injection case.
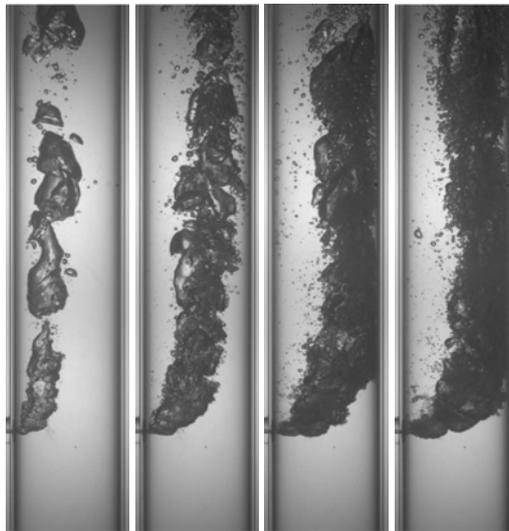
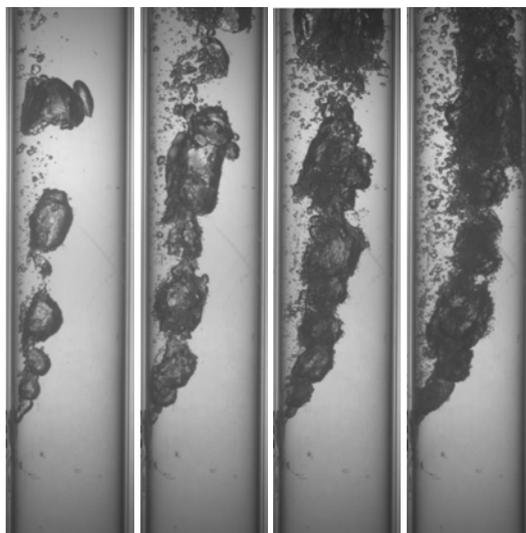Figura 6: General flow configuration for orthogonal injection. $Q_l = 5$ m^{3}h^{-1} and $Q_g = 1, 2, 3$ and 4 m^{3}h^{-1}.

Figura 7: General flow configuration for co-current injection. $Q_l = 5$ m^{3}h^{-1} and $Q_g = 1, 2, 3$ and 4 m^{3}h^{-1}.

4. PRESSURE DROP

The data on pressure drop is shown in Figs. 8 and 9. From the results, it is evident that for a fixed Q_l the increase of Q_g provokes a decrease in ΔP, as expected. For a fixed Q_g, an increase of Q_l increase ΔP.

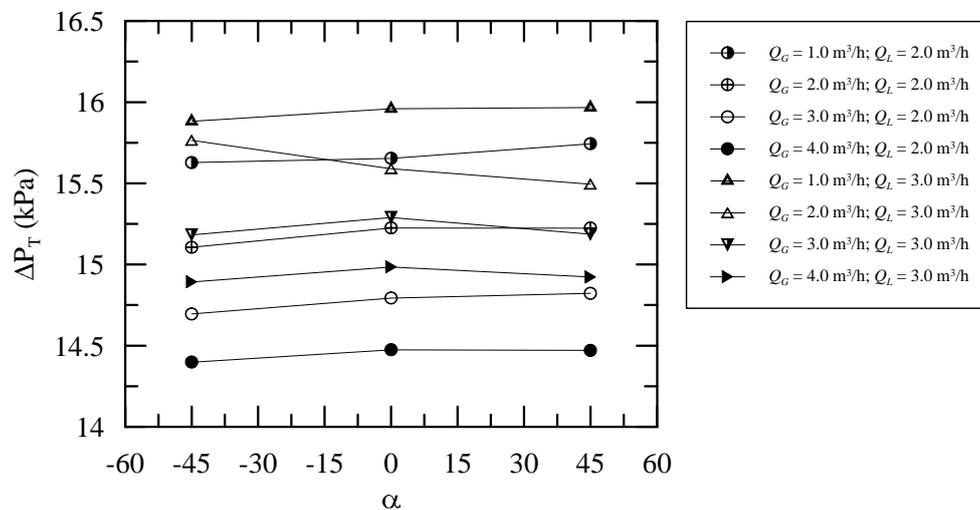The changes resulting from changes in α, however, are not easy to interpret.

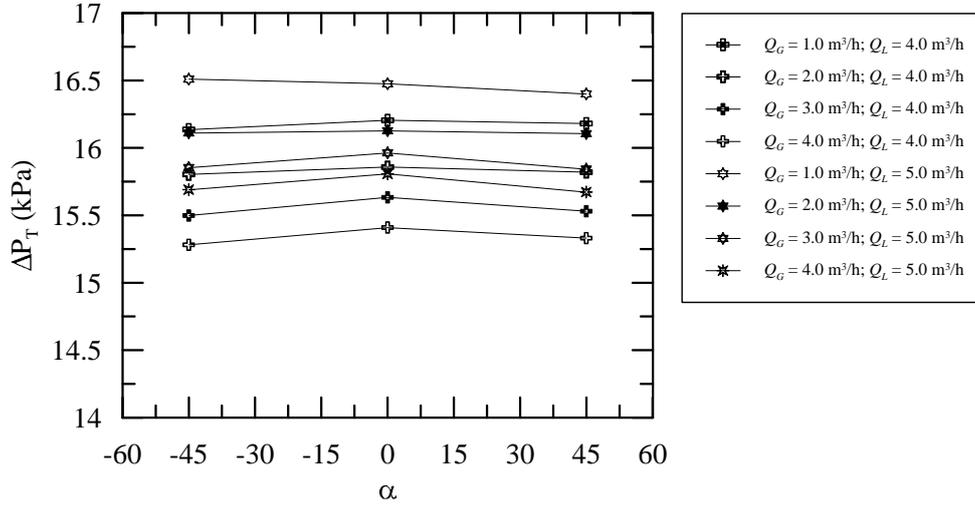Figura 8: Total pressure drop for $Q_l = 2, 3$ m^{3}h^{-1}.

4

Figura 9: Total pressure drop for $Q_l = 4, 5 \ \text{m}^3\text{h}^{-1}$.

As previously discussed the total changes in pressure result from a combination of effects:

$$\Delta P_{Total} = \Delta P_{Gravity} + \Delta P_{Friction} + \Delta P_{Acceleration} + \Delta P_{Turbulence} \tag{1}$$

The gravitational effect is the hydrostatic pressure in the column between the two points where pressure readings are collected; it is a direct result of the fraction volumes of liquid and gas between the two considered positions.

The friction component results from the energy loss at the wall due to viscous effects. Normally in literature this term is estimated accordingly to

$$\Delta P_{Friction} = f \frac{L}{D} \rho_m U_m^2 \tag{2}$$

where L is the length of the pipe, ρ_m is the average density of the mixture and U_m is the mixture velocity.

The friction factor f is determined through empirical correlations based on some appropriate Reynolds number definition.

The acceleration term depends on the velocity and direction of the injected gas. It cannot be confused with the losses provoked by turbulent agitation, bubble break up and coalescence. In fact, $\Delta P_{Acceleration}$ can be determined from a simple momentum balance. The estimation of $\Delta P_{Turbulence}$, however, cannot be obtained from direct measurements. This is a term that needs to be estimated indirectly from Eq. (1).

Figures 8 and 9 show that normally the lowest pressure drop is obtained for $\alpha = -45^o$. The differences between the results obtained for all three injection angles, however, are small. In particular, it appears that for conditions where $Q_l = 4, 5 \ \text{m}^3\text{h}^{-1}$ the condition $\alpha = 0^o$ furnishes the highest pressure drops.

The flow configurations shown in Figs. (2) through (7) suggest that for $\alpha = -45^o$ the amount of resident gas in the test cell (the volume limited by the two pressure taps) is much larger as compared to the other angles of release. The same figures, however, also suggest that the losses due to flow acceleration and turbulence are also the highest for the -45° angle. The implication is that these two effects compensate each other yield a total combined pressure loss that does not change much for different angles.

The losses due to gravitational effects are shown in Figs. 10 and 11. The figures suggest that orthogonal injection results in the highest gravitational pressure losses, that is, less gas is trapped in the test cell. The apparent structural organization of the gas stream reduces the acceleration time of the orthogonal jet resulting in the highest pressure head.

The acceleration and turbulent losses are shown in Fig. 12. As previously mentioned, the orthogonal configuration seems to furnish the lowest aggregate acceleration and turbulent effect.

5. CONCLUSION

The work has studied the effects of the gas orientation on the pressure drop of two-phase upward flow. The results have successfully separated the different contributions on pressure loss, analyzing in particular the relative importance of the gravitational and acceleration (including turbulence) effects. Despite the large losses due to the latter effects, it has been demonstrated that the largest gas hold up resulting from the counter-current angle of injection results in the lowest pressure drop.

New experiments on the local features of the flows are currently under conduction. The experiments hope to report on the bubble diameter distribution, bubble velocities and properties of the continuous phase.
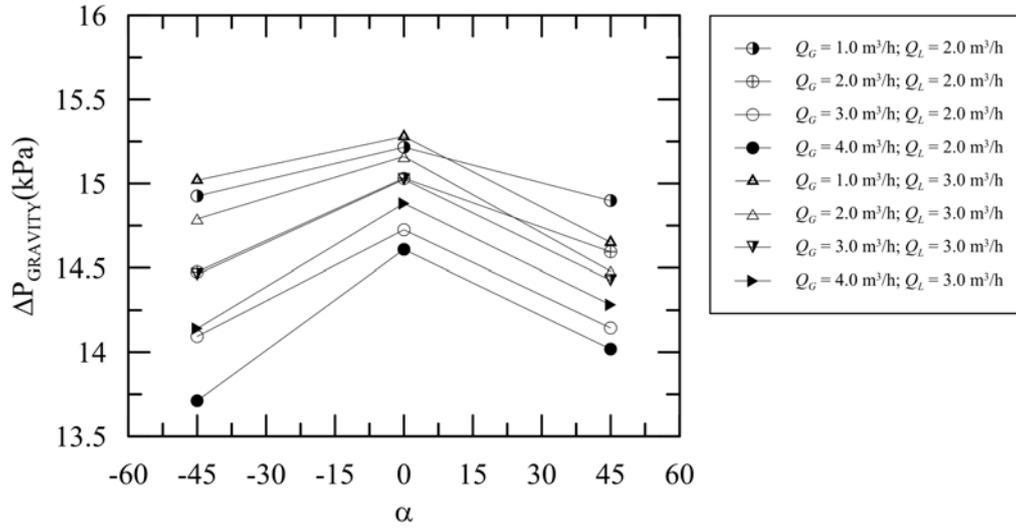
Figura 10: Gravity pressure drop for Q_l = 2, 3 m^{3}h^{-1}.

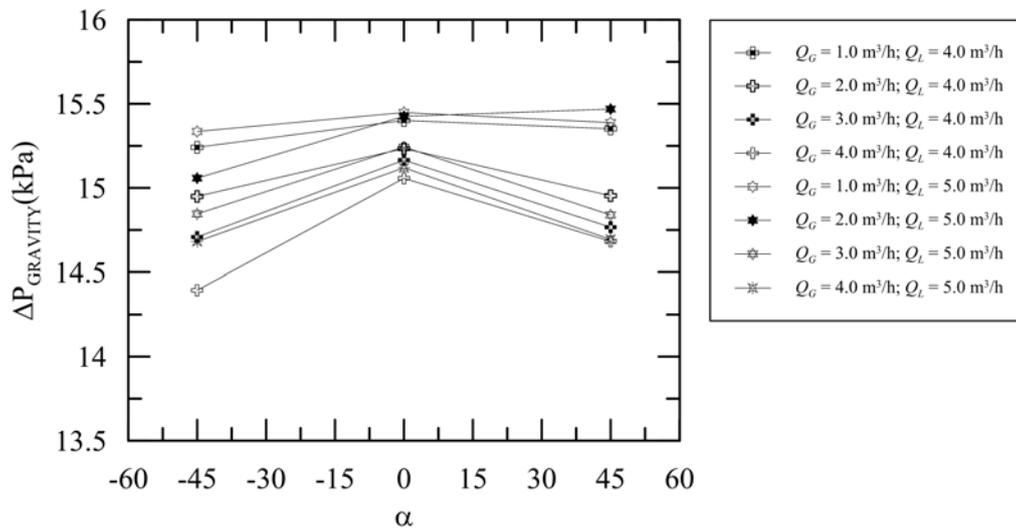Figura 11: Gravity pressure drop for Q_l = 4, 5 m^{3}h^{-1}.
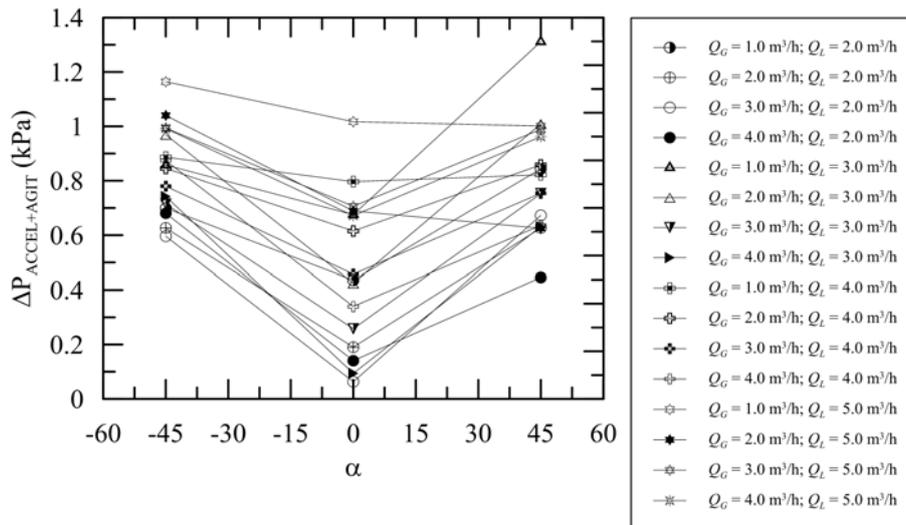
Figura 12: Acceleration and turbulence pressure drop for all flow conditions.

6. ACKNOWLEDGEMENTS

7. REFERENCES

Guet, S., 2004, Bubble Size Effect on the Gas-lift Technique, PhD Thesis, Technische Universiteit Delft.

Saepudin, D., Soewono, E., Sidarto, K.A., Gunawan, A.Y., Siregar, S. and Sukarno, P., 2007, An Investigation on Gas Lift Performance Curve in an Oil-Producing Well, Int. J. Math. & Math. Sci. 15, doi:10.1155/2007/81519.

Brauner, N., 1998. Liquid-liquid two-phase flow. HEDU - Heat Exchanger Design Update, 1-40, chapter 2.3.5.

Descamps, M., Oliemans, R.V.A., Ooms, G., Mudde, R.F., Kusters, R., 2006. Influence of gas injection on phase inversion in an oil-water flow through a vertical tube. Int. J. Multiphase Flow 32, 311-322.

8. RESPONSIBILITY NOTICE

The authors are the only responsible for the printed material included in this paper.